Strong N−H···π Hydrogen Bonding in Amide−Benzene Interactions

Philipp Ottiger, Chantal Pfaffen, Roman Leist, and Samuel Leutwyler*

Departement für Chemie and Biochemie, Universität Bern, Freiestrasse 3, CH-3012 Bern, Switzerland

Rafał A. Bachorz and Wim Klopper*

Center for Functional Nanostructures (CFN) and Institut für Physikalische Chemie, UniversitätKarlsruhe (TH), D-76128 Karlsruhe, Germany

Received: December 15, 2008

Among the weak intermolecular interactions found in proteins, the amide N−H···π interaction has been widely observed but remains poorly characterized as an individual interaction. We have investigated the isolated supersonic-jet-cooled dimer of the *cis*-amide and nucleobase analogue 2-pyridone (2PY) with benzene and benzene-d_6. Both MP2 and SCS-MP2 geometry optimizations yield a T-shaped structure with a N−H···π hydrogen bond to the benzene ring and the C═O group above, but far from the C−H bonds of benzene. The CCSD(T) calculated binding energy at the optimum geometry is D_e = 25.2 kJ/mol (dissociation energy D_0 = 21.6 kJ/mol), corresponding to the H-bond strength of the water dimer or of N−H···O hydrogen bonds. The T-shaped geometry is supported by the infrared−ultraviolet depletion spectra of 2PY·benzene: The N−H stretch vibrational frequency is lowered by 56 cm^{-1}, and the C═O stretch vibration is lowered by 10 cm^{-1}, relative to those of bare 2PY, indicating a strong N−H···π interaction and a weak interaction of the C═O group. The benzene C−H infrared stretches exhibit very small shifts ($\approx$2 cm^{-1}) relative to benzene, signaling the absence of interactions with the benzene C−H groups. The infrared spectral shifts are consistent with a strong nonconventional π hydrogen bond and a T-shaped structure for 2PY·benzene. Symmetry-adapted perturbation theory calculations show that the N−H···π interaction is by far the dominant stabilization factor.

1. Introduction

Nonconventional hydrogen bonds between X−H donors (X = N, O, S) and the π-electron cloud of an aromatic moiety are well documented in structural organic chemistry[1,2] and have been shown to be of great importance in structural biology.[2−7] Amino and amide···π aromatic interactions have been established through data-mining studies of protein crystal structures, in which amine (lysine, arginine) or amide (asparagine = Asn, glutamine = Gln) side chains have been found to pack close to aromatic rings.[3−6,8,9] Steiner and Koellner have reviewed X-ray data on N−H···π and other X−H hydrogen bonds with π-acceptors in proteins,[4] noting that about 1 out of 11 aromatic side-chains accepts a π-hydrogen bond from an X−H donor. They list more than 1300 π-acceptor hydrogen bonds, of which 341 involve phenylalanine (Phe) as acceptor. 239 donor interactions were found with peptide N−H groups, which are available for H-bonding at the ends and edges of sheets and at the N-termini of helices; the corresponding N−H···π interactions are found to be involved in edge and terminus stabilization. A further 130 interactions involve Asn or Gln amide groups as H-donors.[4]

Amide···π interactions are important in the interaction of acetylated lysine (KAc) with highly conserved aromatic residues in the bromodomain,[6] which is a protein domain found in most acyltransferases and in proteins associated with the regulation of chromatin structure. Amide-π interactions have been identified in drug binding to human deoxyhemoglobin,[8] in binding of other ligands to enzymes,[9] and have also been utilized in the selective binding of guests by model systems in organic solution.[10,11]

A prototype for an N−H···π interaction is the complex formed between ammonia and benzene.[12−14] Its experimental gas-phase dissociation energy is D_0 = 7.70 ± 0.50 kJ/mol,[13] close to the value derived from CCSD(T) calculations (D_0 = 6.74 kJ/mol).[15] Another system that involves a significant N−H···π interaction is the pyrrole dimer.[16−18] It has a strongly slanted T-shaped geometry, with a 55° angle between the two pyrrole planes,[16] reflecting a competition between π-stacking and N−H···π hydrogen bond interactions.[16,18] A model for the aromatic−amide (peptide backbone) interaction found in proteins is provided by the formamide−benzene complex. Computational studies of the orientation dependence and the magnitude of the formamide···π interaction have been performed by Duan et al. using second-order Møller−Plesset perturbation (MP2) theory.[5] They predict that T-shaped geometries are more stable than parallel or displaced parallel geometries, the calculated MP2 binding energies are in the range of D_e = 16−17 kJ/mol.[5] The interactions between aromatic rings and backbone amide N−H groups in solution have been investigated by classical MD simulations of a model tripeptide.[7]

The 2-pyridone (2PY) molecule is a six-ring *cis*-amide with neighboring N−H and carbonyl groups[19,20] and can serve as a mimic of uracil and/or thymine,[19−32] which exhibit two sets of neighboring N−H and C═O groups. *Cis*-amides are common in biologically important molecules and significantly influence the structures of nucleic acids, proteins, and peptides. Previously, we have experimentally and theoretically investigated the competition between hydrogen bonding and π-stacking in dimers

* To whom correspondence should be addressed. E-mail: leutwyler@iac.unibe.ch.

10.1021/jp8110474 CCC: $40.75
Published on Web 02/10/2009

of 2PY with fluorobenzenes (*n*FB) with $n = 1-6$.[31−34] The fluorobenzenes with one to five F atoms form doubly hydrogen-bonded complexes with nonconventional N−H···F−C and C−H···O=C hydrogen bonds.[31−33] The exception is 2PY·hexafluorobenzene: since here only a single N−H···F−C hydrogen bond can potentially be formed, the 2-pyridone reorients into a π-stacked geometry.[33,34]

The 2PY·benzene complex is paradigmatic for the interaction of a *cis*-amide with benzene. On the basis of expectations from the 2PY·fluorobenzenes, the benzene molecule might be expected to form a C−H···O=C hydrogen bond, with a secondary C−H···π interaction to the 2PY moiety. Alternatively, a displaced parallel π-stacked geometry is conceivable, as observed for 2PY·hexafluorobenzene[33,34] and as predicted by high-level calculations for the benzene dimer.[35−38] By combining experimental infrared (IR) and ultraviolet (UV) spectra of supersonic-jet-cooled 2PY·benzene and 2PY·benzene-d_6 with high-level ab initio methods, we show here that the ground-state geometry of 2PY·benzene in fact corresponds to a T-shaped structure. We provide an analysis of the relative importance of the N−H···π and C=O···benzene interactions based on IR spectral shifts, in combination with symmetry-adapted perturbation theory (SAPT) calculations. These provide clear evidence that the N−H···π nonconventional hydrogen bond is the dominant interaction and is of comparable strength to a conventional hydrogen bond.

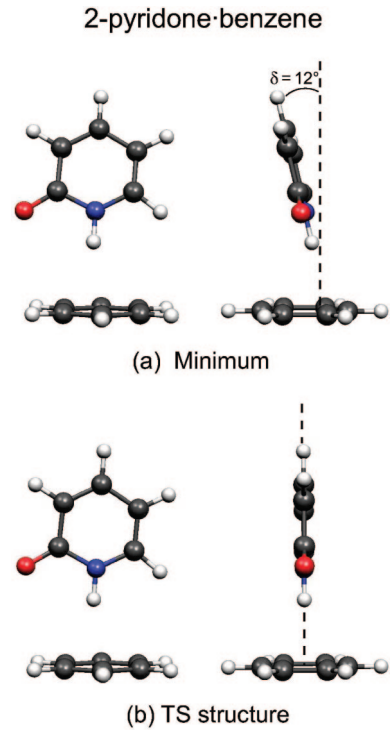

Figure 1. (a) Minimum and (b) TS structure of 2-pyridone·benzene, optimized at the SCS-MP2 level with the aug-cc-pVTZ basis set.

2. Methods

2.1. Calculations. Starting from different trial geometries including hydrogen-bonded and π-stacked structures, the ground-state minimum and transition-state (TS) structures of 2-pyridone·benzene were optimized using the resolution-of-identity second-order Møller−Plesset method (MP2) as well as the spin-component scaled[39] (SCS) MP2 methods with the aug-cc-pVTZ basis set. For the SCS-MP2 calculations, the like and unlike spin components of the MP2 energy were scaled according to recent work by Grimme.[39] The minimum geometry optimization was carried out without any symmetry constraints, whereas the TS optimization was performed within a C_s symmetry restriction.

Binding energies and counterpoise corrections of the minimum and TS structures of 2PY·benzene were then calculated at the CCSD(T) level by adding the contributions from different levels of theory. The HF, MP2, SCS-MP2, MP2-R12,[40] and SCS-MP2-R12[34] contributions were computed with the aug-cc-pVQZ basis set. The CCSD and (T) contributions were obtained with the aug-cc-pVDZ basis set. The computational procedure chosen in the present work is identical to that in refs 33 and 34 except that the unmodified aug-cc-pVDZ basis set was used to compute the (T) contributions, whereas a modified basis (denoted aug-cc-pVDZ′) was used in refs 33 and 34 for these connected triple excitations. Supplementary DFT calculations were performed with the PW91 and B3LYP functionals, using the 6−311++G(d,p) basis set.

Normal mode analyses were carried out at the PW91/6−311++G(d,p), harmonic and anharmonic B3LYP/6−311++G(d,p), MP2/cc-pVDZ, and SCS-MP2/aug-cc-pVDZ levels of theory. The calculations were performed using the programs Gaussian03,[41] Turbomole (RICC2 module),[42] or Molpro.[43]

2.2. Experimental. 2-Pyridone·benzene complexes were synthesized and cooled in a 20 Hz pulsed supersonic jet expansion, using neon as a carrier gas (0.8−1 bar). 2-Pyridone (Aldrich, 97%) was heated to 80−90 °C in the sample holder of the pulsed nozzle. Benzene (Fluka, 99%) or benzene-d_6 (Cambridge Isotopes, 99.5% isotopic purity) was seeded into the neon carrier gas at 2 mbar partial pressure (−35 °C). Mass-selected two-color resonant two-photon ionization (2C-R2PI) spectra were recorded over the 29 000−31 500 cm^{-1} spectral range. The $S_0 \rightarrow S_1$ excitation was performed by a frequency-doubled DCM dye laser (pulse energy 160 μJ), and the fourth harmonic (266 nm) of the same Nd:YAG laser was used for ionization (pulse energy 500 μJ). The ions were separated in a time-of-flight (TOF) mass spectrometer and detected by double multichannel plates.

Mass-selected infrared (IR) depletion spectra were measured over the 1400−2000 cm^{-1} and 2700−3600 cm^{-1} ranges. These were recorded by monitoring the depletion of the 2C-R2PI ion signal when tuning the infrared frequency, with the UV excitation wavelength fixed to the respective electronic origins of the $S_0 \rightarrow S_1$ transition (see below). Alternate UV laser pulses were preceded by 100 ns with an IR laser pulse (8−14 mJ/pulse) generated by a 10 Hz Laser Vision OPO/OPA system. For the 1400−2000 cm^{-1} range, the signal and idler outputs of the OPA were mixed in an $AgGaSe_2$ crystal to produce ≈1.5 mJ of mid-IR radiation. The IR beam was focused by a CaF_2 lens and overlapped anticollinearly with the UV laser pulses in the TOF mass spectrometer source. The IR wavenumber scale was calibrated against a photoacoustic H_2O vapor spectrum recorded synchronously with each scan.

3. Results and Discussion

3.1. Geometry Optimization and Binding Energies. The ground-state optimizations of 2PY·benzene at the MP2 and SCS-MP2 levels with the aug-cc-pVTZ (aVTZ) basis set both result in tilted T-shaped structures with an N−H···π interaction from the 2-pyridone moiety to the benzene ring. The MP2 method predicts the plane of 2PY to be tilted by $\delta = 38°$ relative to the surface normal of benzene, whereas the SCS-MP2 method gives a smaller tilt angle of $\delta = 12°$, see Figure 1a. The asymmetry of the T-shaped structure implies two enantiomeric

TABLE 1: Geometry Parameters for the MP2 and SCS-MP2 Optimized Structures of 2-Pyridone·Benzene with the aug-cc-pVTZ Basis Set

	SCS-MP2		MP2	
	minimum	TS struct.	minimum	TS struct.
tilt angle δ/°	12.4	0.00	38.1	0.00
$R_{cm,vert}$/Å	4.27	4.32	3.88	4.21
$R_{cm,horiz}$/Å	0.54	0.49	0.93	0.44
2PY N···Bz plane/Å	3.19	3.21	3.02	3.10
2PY N−H···Bz plane/Å	2.20	2.20	2.19	2.09
2PY C═O···Bz plane/Å	3.24	3.28	2.96	3.15

minimum-energy structures that are interconverted by the intermolecular tilting mode (denoted δ), via the T-shaped C_s-symmetric TS structure, see Figure 1b. The PW91 and B3LYP DFT calculations yielded T-shaped structures that are qualitatively similar to the MP2 and SCS-MP2 geometries. The vertical and horizontal displacement between the two centers of mass, $R_{cm,vert}$ and $R_{cm,horiz}$, as well as the distances from the molecular plane of benzene to the N, the H-bonded H atom, and the carbonyl O atom are summarized in Table 1 for the MP2 and SCS-MP2/aVTZ minima.

At the MP2 optimum, the 2PY moiety is considerably closer to the benzene plane than at the SCS-MP2 optimum geometry, the N···benzene and the $R_{cm,vert}$ distances being 0.17 and 0.39 Å shorter, respectively. However, these result from the larger tilt angle of the MP2 structure. The distance from the H atom of the N−H group to the benzene plane is nearly the same, being 2.20 Å (SCS-MP2) and 2.19 Å (MP2), respectively. Both these N−H···benzene distances are about 0.3 Å shorter than the C−H···benzene distance in the T-shaped benzene dimer, based on the structure optimized by Janowski and Pulay at the QCISD(T)/aug-cc-pVTZ level.[35] This directly reflects the much larger interaction strength of the 2-pyridone moiety compared to benzene when acting in the same H-donor geometry, see also below. Interestingly, the N−H bond length decreases very slightly from 1.020 Å in bare 2PY to 1.016 Å in 2PY·benzene, whereas the C═O bond length increases from 1.225 to 1.235 Å upon complexation.

At the MP2 and SCS-MP2 optimized minimum and TS structures, the binding energies were recalculated using the larger aug-cc-pVQZ basis set and adding the R12, CCSD, and (T) contributions. For the different minimum and TS structures, the BSSE at the CCSD(T) = HF + MP2 + R12 + CCSD + (T) level is nearly constant at 1.4−1.6 kJ/mol. The final raw and counterpoise (CP)-corrected binding energies are given in Table 2. The CCSD(T) counterpoise-corrected binding energy is D_e = 25.2 kJ/mol at the SCS-MP2 optimized structure and 23.9 kJ/mol at the MP2 structure. These values can be compared to the binding energy of the benzene dimer, D_e = 11.0 kJ/mol, optimized at the QCISD(T)/aug-cc-pVQZ level by Janowsky and Pulay.[35]

The CP-corrected CCSD(T) racemization barrier, that is, the energy differences between the enantiomeric SCS-MP2 minima and the TS structure is very small, being 0.08 kJ/mol. The barrier for rotation of benzene around its local C_6 axis is also low, being 0.19 kJ/mol at the MP2 and 0.16 kJ/mol at the SCS-MP2 levels. Thus, the benzene moiety can be viewed as a nearly free internal rotor, as in the benzene dimer.[35−38] Since the CCSD(T) calculation gives a larger binding energy for the SCS-MP2 optimized geometry than for the MP2 structure—both at the counterpoise-corrected and noncounterpoise-corrected levels—we consider the SCS-MP2 structure to be closer to the true minimum energy structure.

3.2. Resonant Two-photon Ionization Spectra and IR−UV Depletion Spectra. The 2C-R2PI spectra of 2PY·benzene and 2PY·benzene-d_6 are presented in Figure 2.

The 0_0^0 bands of the $S_0 \rightarrow S_1$ transitions are assigned to the intense bands at 29 730 (2PY·benzene) and 29 732 cm^{-1} (2PY·benzene-d_6). Full deuteration of the benzene has little influence on the 2C-R2PI spectrum; the origin is shifted 2 cm^{-1} to the blue, and the band structure remains nearly identical. The vibronic spectrum is rather complicated; we have tentatively assigned the band structure in terms of a very low-frequency δ tilting vibration (see above), three (nearly) symmetric intermolecular vibrations, and intramolecular out-of-plane excitations of the 2PY moiety. A detailed analysis will be presented elsewhere. We note that the spectra in Figure 2 are very different from those typically observed for doubly hydrogen-bonded 2PY complexes,[31−33] showing that the intermolecular interaction is not of the classical H-bond type.

The N−H, C═O, and C−H stretching frequencies provide sensitive diagnostics of the intermolecular interactions. Figure 3 shows the infrared depletion spectra of 2PY, 2PY·benzene, and 2PY·benzene-d_6 measured over the 2800−3600 cm^{-1} range. The single intense band of 2PY at 3448 cm^{-1} corresponds to the N−H stretch.[22,44] In the spectra of 2PY·benzene and 2PY·benzene-d_6, this band is shifted by −56 cm^{-1} to 3392 cm^{-1}. This assignment is in good agreement with the anharmonic B3LYP and scaled MP2 frequencies listed in Table 3 and shown in Figure 4 below. The spectral red shift relative to the N−H stretch mode of the 2PY monomer indicates that there is a significant H-bond interaction between the N−H group of 2PY and the benzene (or benzene-d_6) moiety.

Closely above the N−H stretch bands of 2PY·benzene and 2PY·benzene-d_6, lower intensity bands are observed at 3409 cm^{-1} that do not occur in the spectrum of bare 2PY. They arise from Fermi resonances of the C═O stretch overtones with the close-lying intense N−H stretch of 2PY. The C═O stretch fundamental of 2PY·benzene is discussed below.

In the 2PY·benzene spectrum, three bands appear in the 2900−3200 cm^{-1} range, see Figure 3b. Due to their complete absence in the 2PY·benzene-d_6 spectrum, Figure 3c, they are assigned to the three IR transitions of benzene that lie in this range.[45−48] The moderately intense band at 3046 cm^{-1} is assigned as the ν_{20} (e_{1u}) fundamental (3048 cm^{-1} in benzene). The intense band at 3077 cm^{-1} is attributed to the $\nu_1 + \nu_6 + \nu_{19}$ combination band (3079 cm^{-1} in benzene) and the weaker band at 3099 cm^{-1} to the $\nu_8 + \nu_{19}$ combination (3101 cm^{-1} in benzene). All three IR-active C−H vibrations of the bare benzene are also observed in 2PY·benzene. However, they are shifted by only −2 cm^{-1} upon complexation with the amide, implying that there is no intermolecular interaction of the C−H oscillators with the 2PY moiety.

In Figure 4, the experimental IR spectrum is compared to the IR spectra calculated at the harmonic PW91/6−311++G(d,p), MP2/cc-pVDZ, and SCS-MP2/aVDZ levels and at the anharmonic B3LYP/6−311++G(d,p) level. The calculated frequencies and intensities are indicated as stick-plots. The unscaled PW91 harmonic frequencies are useful in the hydride stretch range, the N−H stretch is predicted only 37 cm^{-1} (1.1%) too high.[29] The MP2 and SCS-MP2 harmonic frequencies were scaled by the factors 0.954 and 0.957, respectively, as calibrated previously;[34] they agree with experiment to within 12 cm^{-1} in the N−H and C−H stretching regions. Very good agreement with the experimental frequencies is also obtained at the second-order perturbative (PT2) anharmonic B3LYP level of theory (based on third and semidiagonal fourth derivatives). Because

TABLE 2: Binding Energies D_e and Dissociation Energies D_0 (Including Counterpoise Corrections) of the Minimum and TS Structures of 2-Pyridone·Benzene (in kJ/mol)

	SCS-MP2		MP2	
	minimum	TS struct.	minimum	TS struct.
		Noncounterpoise-corrected		
HF + MP2 + R12[a]	31.12	30.88	31.92	30.94
HF + SCS-MP2 + R12[a]	23.63	23.56	22.21	22.46
HF + MP2 + R12 + CCSD + (T)[b]	26.58	26.50	25.50	25.71
		Counterpoise-corrected		
HF + MP2 + R12[a]	30.44	30.20	31.15	30.20
HF + SCS-MP2 + R12[a]	22.94	22.88	21.43	21.71
HF + MP2 + R12 + CCSD + (T)[b]	25.20	25.12	23.90	24.22
zero-point vibrational energy contribution	− 3.58	− 3.51	− 3.44	− 3.33
dissociation energy D_0, CCSD(T)	21.62	21.61	20.46	20.89

[a] Optimized with the aug-cc-pVTZ basis set, energies with the aug-cc-pVQZ basis set. [b] CCSD and (T) contributions obtained with the aug-cc-pVDZ basis set.

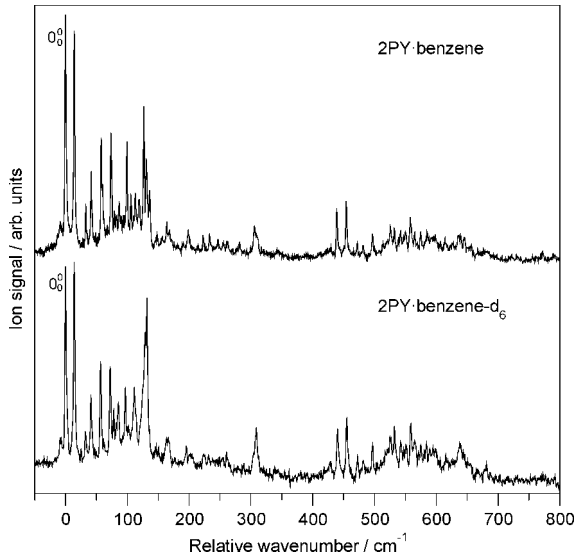

Figure 2. Two-color resonant two-photon ionization spectra of 2-pyridone·benzene and 2-pyridone·benzene-d_6. The wavenumber scale is relative to the $S_0 \rightarrow S_1$ origins.

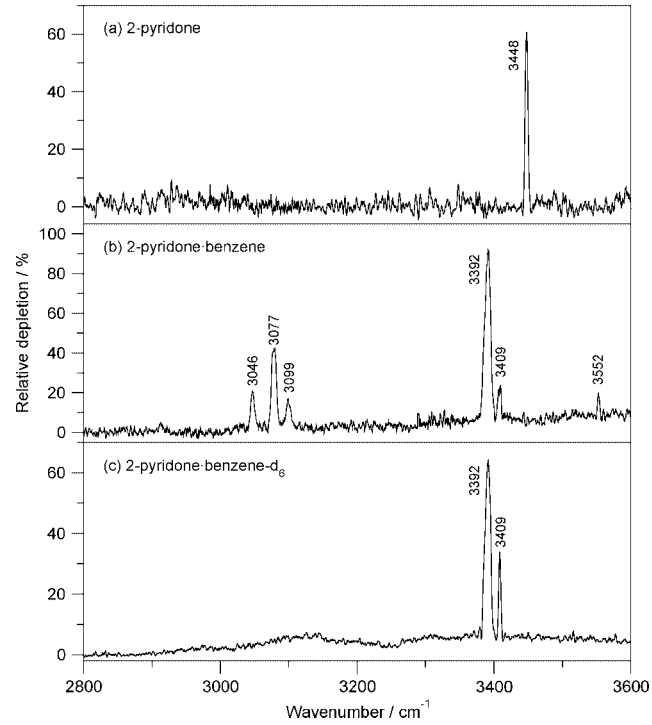

Figure 3. Infrared depletion spectra of 2-pyridone, 2PY·benzene, and 2PY·benzene-d_6 in the C−H and N−H stretching frequency range, with R2PI detection at the 0_0^0 bands, see Figure 2.

the anharmonic calculations do not give IR intensities, the B3LYP harmonic intensities are shown in Figure 4 as qualitative indicators. The N−H stretch is predicted only 18 cm^{-1} (0.5%) too low, and the benzene e_{1u} fundamental is only 26 cm^{-1} (0.8%) too high.

The shifts of the experimental N−H stretch frequencies for a series of 2-pyridone complexes are compared in Figure 5 as a function of the respective MP2/aug-cc-pVTZ calculated binding energies.

The intermolecular interactions involved range from weak N−H···F−C hydrogen bonds in 2PY·fluorobenzene and 2PY·1,4-difluorobenzene, to 2PY·H_2O, which has a cyclic H-bonding topology with an N−H···OH_2 and an HO−H···O═C hydrogen bond, to $(2PY)_2$ with two strong N−H···O═C hydrogen bonds. For the latter dimer, the N−H···O═C hydrogen bond strength is ≈42 kJ/mol, which is about 12% of the N−H chemical bond energy. The large external perturbation by the H-bond, combined with the comparatively large change of effective reduced mass for the N−H stretch upon complex formation lead to the nonlinearity of the plot. The N−H frequency shift of −56 cm^{-1} for 2PY·benzene is characteristic for a medium-strength hydrogen bond, being smaller than that of N−H···O−H_2 in the 2PY·H_2O complex, but is larger than that observed for the N−H···F−C hydrogen-bonded complexes.

The third important diagnostic for intermolecular interactions in this complex is the C═O stretching frequency. Figure 6 shows the mass-specific IR depletion spectra of 2-pyridone, 2PY·benzene, and 2PY·benzene-d_6 between 1200−2000 cm^{-1}.

All three spectra show a single intense band corresponding to the C═O stretch of 2-pyridone, which lies at 1724 cm^{-1} for 2PY and is shifted 10 cm^{-1} to lower frequency for 2PY·benzene and 2PY·benzene-d_6. A further comparison for the C═O frequency shift is afforded by the IR spectrum of 2PY·H_2O, Figure 6. Here, the C═O stretch is shifted farther, to 1711 cm^{-1}, the 1598 cm^{-1} band is due to the H−O−H bend of the water moiety.

The experimental C═O frequency shifts for these 2-pyridone complexes are compared in Figure 7 as a function of the MP2/aug-cc-pVTZ calculated binding energies. The change of the C═O stretching frequency as a function of hydrogen bond strength is 10−20 times smaller than for the N−H stretches. The main reasons for this are that (i) even for the largest N−H···O═C interaction in $(2PY)_2$ (≈42 kJ/mol), the external

TABLE 3: Experimental and Calculated Vibrational Stretching Frequencies (in cm^{-1}) and Intensities (in parentheses, km/mol) of 2-Pyridone·Benzene, 2-Pyridone·Benzene-d_6, and 2-Pyridone

	2-pyridone·benzene				2-pyridone·benzene-d_6			
mode	exp	B3LYP[a] anharm.	PW91[a]	MP2[b]	exp	B3LYP[a] anharm.	PW91[a]	MP2[b]
Benzene								
b_{1u} stretch		3131.6	3099.4 (0.5)	3063.9 (0.1)		2243.9	2283.3 (0.3)	2263.7 (0.0)
$e_{2g,a}$ stretch		3037.0	3108.3 (0.8)	3074.6 (2.2)		2257.9	2293.2 (0.3)	2276.7 (0.8)
$e_{2g,b}$ stretch		3048.6	3111.4 (6.5)	3081.0 (8.2)		2262.8	2296.2 (2.8)	2282.1 (2.1)
$e_{1u,a}$ stretch	3046	3072.2	3123.3 (26.5)	3091.1 (9.1)		2268.0	2312.3 (14.9)	2298.2 (7.1)
$e_{1u,b}$ stretch		3075.2	3124.7 (12.4)	3095.9 (9.3)		2271.5	2313.4 (7.2)	2299.3 (8.1)
a_{1g} stretch		3056.1	3133.0 (2.7)	3108.3 (0.9)		2289.6	2324.2 (1.4)	2313.5 (0.4)
2PY moiety								
C═O stretch	1714	1702.8	1693.3 (541)	1709.0 (385)	1714	1702.7	1693.2 (542)	1709.0 (386)
N−H stretch	3392	3373.8	3429.4 (395)	3404.2 (317)	3386	3373.8	3429.3 (395)	3404.1 (316)
2·C═O stretch	3409	3393.1			3402	3392.9		
2-Pyridone								
C═O stretch	1724	1709.6	1703.7 (606)	1725.2 (451)				
N−H stretch	3448	3423.2	3511.4 (50.9)	3448 (70.6)				

[a] 6−311++G(d,p) basis set. [b] cc-pVDZ basis set; scaling factor 0.954.

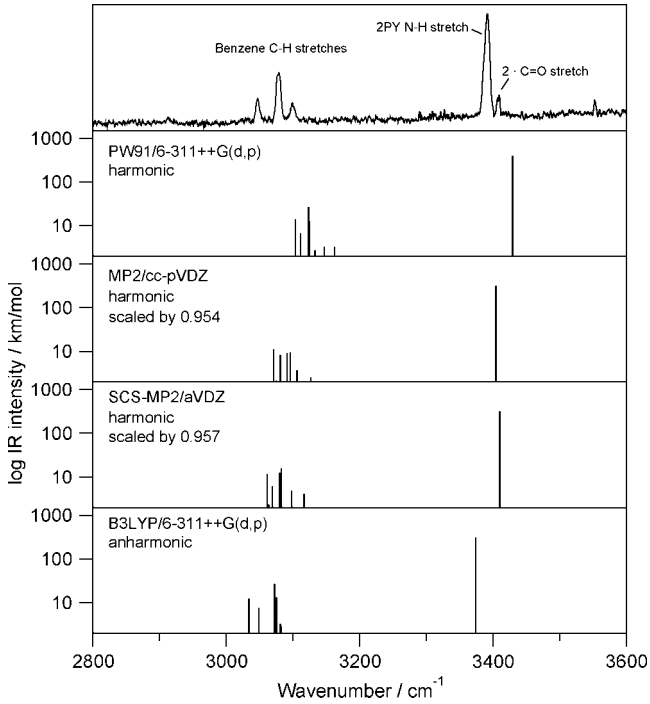

Figure 4. IR/UV-depletion spectrum of 2PY·benzene, compared to the PW91/6−311++G(d,p), MP2/cc-pVDZ, SCS-MP2/aVDZ, and anharmonic B3LYP/6−311++G(d,p) calculated frequencies.

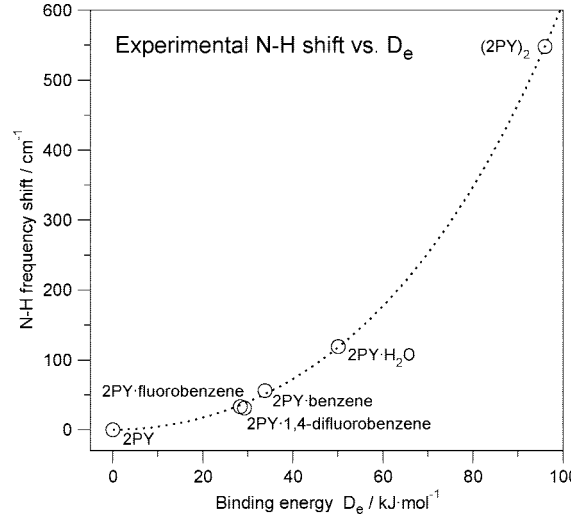

Figure 5. Experimental N−H stretching frequencies of 2-pyridone complexes vs the respective MP2/aVTZ calculated binding energies D_e.

perturbation is only about 4% of the C═O bond strength; and (ii) the change of effective reduced mass of the C═O oscillator due to hydrogen bonding is much smaller than for the N−H stretch, due to the 16 times larger mass of the oxygen atom. Therefore, the frequency shifts are much smaller, and the plot is nearly linear, in contrast to Figure 5. For 2PY·benzene, the C═O frequency shift is about two-thirds of that for 2PY·H_2O. This implies that the side-on interaction of the C═O group with the C−H groups of benzene is non-negligible but weaker than that of the HO−H···O═C interaction in the 2PY·H_2O complex. Also, we cannot exclude that there is an indirect contribution to the C═O shift from the N−H···π interaction since the N−H and C═O groups are part of a conjugated ring and are immediately adjacent to each other.

3.3. Interaction Energy Contributions from Symmetry-Adapted Perturbation Theory. To understand how the N−H···π and C═O···H hydrogen bonds contribute to the total interaction energy of 2PY·benzene, symmetry-adapted perturbation theory (SAPT) was used to calculate and compare the contributions to the interaction energies of benzene with 2-pyridone and 4-pyridone (4PY). In the latter, the C═O group of the pyridone moiety is moved from position 2 to 4, see Scheme 1. Otherwise, the pyridone framework geometry was kept identical. A fully relaxed SCS-MP2/aug-cc-pVQZ structure was also calculated for 4PY·benzene. The structural and the energetic changes between the relaxed and nonrelaxed 4PY·benzene complex are very small, ≤0.01 Å and ≤0.5 kJ/mol, respectively.

The SAPT calculations were carried out at the SCS-MP2 geometry with the aug-cc-pVDZ basis, using the Molpro program.[43] The resulting first-order (electrostatic and exchange) and second-order (induction and dispersion) terms are listed in Table 4. The exchange-induction and exchange−dispersion second-order cross terms were combined with the induction and dispersion terms and are denoted E_{ind} and E_{disp} in Table 4.

The SAPT total binding energy for 2PY·benzene is D_e = 21.8 kJ/mol, arising from the combination of a positive (destabilizing) exchange-repulsion component (+34.5 kJ/mol) to the interaction energy and a larger negative (stabilizing) part (−56.3 kJ/mol). Note that the SAPT binding energy lies in between the SCS-MP2 and MP2 binding energies, cf. Table 2.

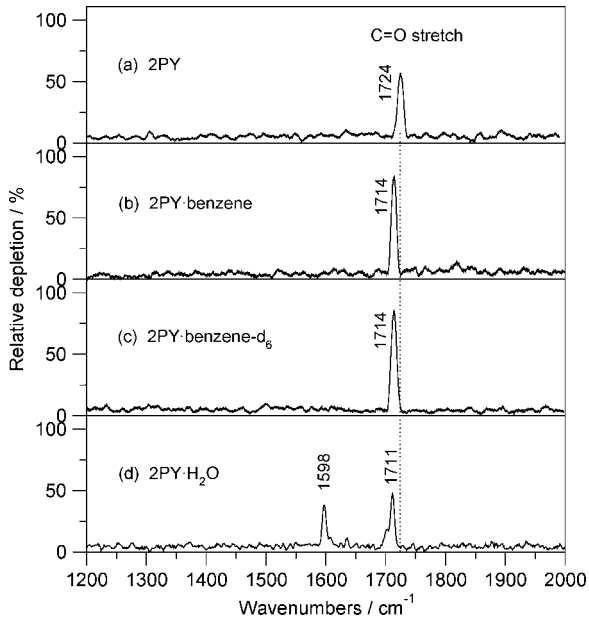

Figure 6. IR/UV-depletion spectra of 2PY, 2PY·benzene, 2PY·benzene-d_6, and 2PY·H_2O in the 1200−2000 cm^{-1} range. R2PI detection at the 0_0^0 bands, see Figure 2a,b.

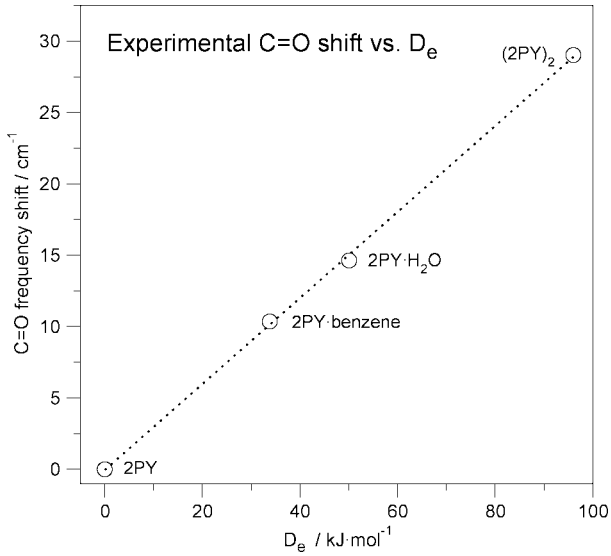

Figure 7. Experimental C═O stretching frequencies of 2-pyridone complexes vs the respective RIMP2/aVTZ calculated binding energies D_e.

SCHEME 1: Orientation of the C═O group of the pyridone moiety

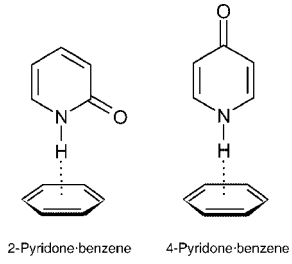

The largest stabilizing SAPT contributions arise from the dispersion (46%) and electrostatic (41%) interactions. The induction energy contribution is smaller, contributing only 13% to the total stabilization.

TABLE 4: Symmetry-adapted Perturbation Theory Interaction Energy Components (in kJ/mol) for the Complexes of Benzene with 2-Pyridone and 4-Pyridone

contribution	2-pyridone·benzene[a]	4-pyridone·benzene[a]
E_{exch}	34.51	31.97
$E_{el\text{-}stat}$	− 23.15	− 23.99
E_{ind}	− 7.17	− 6.56
E_{disp}	− 26.00	− 24.05
total interaction	− 21.81	− 22.63

[a] Destabilizing and stabilizing components are positive and negative, respectively.

Exchanging 2-pyridone by 4-pyridone, that is, moving the carbonyl group to the far side of the pyridone moiety, leads to relatively small changes only: the total SAPT binding energy increases by 4% (0.8 kJ/mol), the electrostatic contribution also increases by 4%, whereas the exchange, induction, and dispersion energies decrease by 7−9%.

The comparison of 2PY·benzene with 4PY·benzene within the framework of the SAPT analysis shows that the 2PY·benzene complex is dominantly stabilized by the nonconventional N−H···π hydrogen bond and that interactions to the C═O group are much less important. The latter are also stabilizing but are mostly due to a small dispersion contribution (≈2 kJ/mol) and a minute inductive contribution (≈0.6 kJ/mol). The existence of a "side-on" C−H···O═C hydrogen bond is not supported by the SAPT calculations, in agreement with the spectroscopic results.

4. Conclusions

As a model for N−H···π and *cis*-amide interactions with the benzene moiety, the 2-pyridone·benzene complex has been studied both experimentally by IR/UV laser spectroscopic methods and by high-level ab initio calculations using the MP2, SCS-MP2, and CCSD(T) methods and large basis sets.

The experimental IR band shifts of the N−H group of the 2-pyridone moiety is −56 cm^{-1}. Although the N−H···π interaction corresponds to a "nonclassical" π-hydrogen bond, both the lowering of the N−H stretch frequency and the IR band intensity increase are signatures of classical hydrogen bonding. The N−H shift of 2-pyridone is also in the range typical for conventionally H-bonded 2PY complexes, lying between the shifts observed for N−H···F−C and N−H···OH_2 hydrogen bonds.

The carbonyl IR band shift is only −10 cm^{-1}, and the shifts of the benzene C−H fundamental and combination bands are insignificant (−2 cm^{-1}). Theory also shows that the C═O···π side-on interaction cannot be characterized as a hydrogen bond, since (i) such a putative H-bond would be very strongly bent; (ii) in the minimum geometry, the C═O group is oriented between the C−H groups of the benzene moiety and not collinear to a C−H group; and (iii) the shift of the C═O group to the para position results in hardly any change of the interaction strength.

Further analysis of the ab initio results using SAPT calculations reveals that the 2PY·benzene complex is dominantly stabilized by the N−H···π hydrogen bond. The electrostatic contribution by the C═O group is close to zero, and the dispersive plus inductive contributions from this group are only ≈3 kJ/mol. Thus, a side-on C−H···O═C hydrogen bond is also not supported by the SAPT analysis.

The ab initio calculations predict a T-shaped interaction geometry with all computational methods and basis sets employed. The tilt angle between the 2-pyridone and the

benzene moieties depends on the basis set, but the tilting barrier at the CCSD(T) level is minute, 0.08 kJ/mol, decreasing to 0.01 kJ/mol when including zero-point vibrational energy corrections. With a CCSD(T) binding energy of $D_e = 25.2$ kJ/mol (dissociation energy $D_0 = 21.6$ kJ/mol) the *cis*-amide···π interaction of 2-pyridone·benzene is very substantial, about 2.5 times larger than that calculated for the T-shaped benzene dimer,[35−38] and 1.5 times larger than that of the formamide···benzene interaction calculated at the MP2 level.[5] In fact, this interaction is comparable to intermediate-strength hydrogen bonds, for example, the water dimer or the N−H···O hydrogen bond that occur widely in proteins.[49−52] This atypically large interaction energy is expected to play a very significant role for our understanding of amid NH···π interactions in biological systems.[2−6,8,53]

Acknowledgment. Financial support from the Schweiz. Nationalfonds through grant No. 200021-102030 is gratefully acknowledged. We thank Dr. J. A. Frey for early contributions to the calculations. The research in Karlsruhe has been supported by the Deutsche Forschungsgemeinschaft through the Center for Functional Nanostructures (CFN, Project No. C3.3). It has been further supported by a grant from the Ministry of Science, Research and the Arts of Baden-Württemberg (Az: 7713.14-300).

References and Notes

(1) Malone, J. F.; Murray, C. M.; Charlton, M. C.; Docherty, R.; Lavery, A. J. *J. Chem. Soc. Far. Trans.* **1997**, *93*, 3429.
(2) Meyer, E. A.; Castellano, R. K.; Diederich, F. *Angew. Chem., Int. Ed.* **2003**, *42*, 1210.
(3) Burley, S. K.; Petsko, G. A. *FEBS Lett.* **1986**, *203*, 139.
(4) Steiner, T.; Koellner, G. *J. Mol. Biol.* **2001**, *305*, 535.
(5) Duan, G.; Smith, V. H.; Weaver, D. F. *J. Phys. Chem. A* **2000**, *104*, 4521.
(6) Hughes, R. M.; Waters, M. L. *J. Am. Chem. Soc.* **2006**, *128*, 13586.
(7) Toth, G.; Murphy, R. F.; Lovas, S. *J. Am. Chem. Soc.* **2001**, *123*, 11782.
(8) Levitt, M.; Perutz, M. F. *J. Mol. Biol.* **1988**, *201*, 741.
(9) Perutz, M. F. *Phil Trans. Roy. Soc. A* **1993**, *345*, 105.
(10) Bisson, A. P.; Lynch, V. M.; Monahan, M. C.; Anslyn, E. V. *Angew. Chem., Int. Ed.* **1997**, *36*, 2340.
(11) Snowden, T. S.; Bisson, A. P.; Anslyn, E. V. *J. Am. Chem. Soc.* **1999**, *121*, 6324.
(12) Rodham, D. A.; Suzuki, S.; Suenram, R. D.; Lovas, F. J.; Dasgupta, S.; Goddard, W. A.; Blake, G. A. *Nature* **1993**, *362*, 735.
(13) Mons, M.; Dimicoli, I.; Tardivel, B.; Piuzzi, F.; Brenner, V.; Millie, P. *Phys. Chem. Chem. Phys.* **2002**, *4*, 571.
(14) Vaupel, S.; Brutschy, B.; Tarakeshwar, P.; Kim, K. S. *J. Am. Chem. Soc.* **2006**, *128*, 5416.
(15) Tsuzuki, S.; Honda, K.; Uchimuri, T.; Mikami, M.; Tanabe, K. *J. Am. Chem. Soc.* **2000**, *122*, 11450.
(16) Columberg, G.; Bauder, A. *J. Chem. Phys.* **1997**, *106*, 504.
(17) Matsumoto, Y.; Honma, K. *J. Chem. Phys.* **2007**, *127*, 184310.
(18) Dauster, I.; Rice, C. A.; Zielke, P.; Suhm, M. A. *Phys. Chem. Chem. Phys.* **2008**, *10*, 2827.
(19) Nimlos, M. R.; Kelley, D. F.; Bernstein, E. R. *J. Phys. Chem.* **1987**, *91*, 6610.
(20) Held, A.; Pratt, D. *J. Am. Chem. Soc.* **1990**, *112*, 8629.
(21) Held, A.; Champagne, B. B.; Pratt, D. *J. Chem. Phys.* **1991**, *95*, 8732.
(22) Nowak, M. J.; Lapinski, L.; Fulara, J.; Les, A.; Adamowicz, L. *J. Phys. Chem.* **1992**, *96*, 1562.
(23) Müller, A.; Talbot, F.; Leutwyler, S. *J. Chem. Phys.* **2000**, *112*, 3717.
(24) Müller, A.; Talbot, F.; Leutwyler, S. *J. Chem. Phys.* **2001**, *115*, 5192.
(25) Borst, D. R.; Roscioli, J. R.; Pratt, D. W.; Florio, G. M.; Zwier, T. S.; Müller, A.; Leutwyler, S. *Chem. Phys.* **2002**, *283*, 341.
(26) Müller, A.; Talbot, F.; Leutwyler, S. *J. Am. Chem. Soc.* **2002**, *124*, 14486.
(27) Müller, A.; Leutwyler, S. *J. Phys. Chem. A* **2004**, *108*, 6156.
(28) Müller, A.; Frey, J. A.; Leutwyler, S. *J. Phys. Chem. A* **2005**, *109*, 5055.
(29) Frey, J. A.; Müller, A.; Frey, H.-M.; Leutwyler, S. *J. Chem. Phys.* **2004**, *121*, 8237.
(30) Frey, J. A.; Müller, A.; Leutwyler, S. *ChemPhysChem* **2006**, *7*, 1494.
(31) Leist, R.; Frey, J. A.; Leutwyler, S. *J. Phys. Chem. A* **2006**, *110*, 4180.
(32) Frey, J. A.; Leist, R.; Leutwyler, S. *J. Phys. Chem. A* **2006**, *110*, 4188.
(33) Leist, R.; Frey, J. A.; Ottiger, P.; Frey, H. M.; Leutwyler, S.; Bachorz, R. A.; Klopper, W. *Angew. Chem., Int. Ed.* **2007**, *46*, 1433.
(34) Bachorz, R. A.; Bischoff, F. A.; Höfener, S.; Klopper, W.; Ottiger, P.; Leist, R.; Frey, J. A.; Leutwyler, S. *Phys. Chem. Chem. Phys.* **2008**, *10*, 2758.
(35) Janowski, T.; Pulay, P. *Chem. Phys. Lett.* **2007**, *447*, 27.
(36) Sinnokrot, M. O.; Sherill, C. D. *J. Phys. Chem. A* **2006**, *110*, 10656.
(37) Podeszwa, R.; Bukowski, R.; Szalewicz, K. *J. Phys. Chem. A* **2006**, *110*, 10345.
(38) Tsuzuki, S.; Honda, K.; Uchimuri, T.; Mikami, M.; Tanabe, K. *J. Am. Chem. Soc.* **2002**, *124*, 104.
(39) Grimme, S. *J. Chem. Phys.* **2003**, *118*, 9095.
(40) Klopper, W.; Manby, F. R.; Ten-no, S.; Valeev, E. F. *Int. Rev. Phys. Chem.* **2006**, *25*, 427.
(41) Frisch, M. J.; Trucks, G. W.; Schlegel, H. B.; Scuseria, G. E.; Robb, M. A.; Cheeseman, J. R.; Montgomery, J. A., Jr.; Vreven, T.; Kudin, K. N.; Burant, J. C.; Millam, J. M.; Iyengar, S. S.; Tomasi, J.; Barone, V.; Mennucci, B.; Cossi, M.; Scalmani, G.; Rega, N.; Petersson, G. A.; Nakatsuji, H.; Hada, M.; Ehara, M.; Toyota, K.; Fukuda, R.; Hasegawa, J.; Ishida, M.; Nakajima, T.; Honda, Y.; Kitao, O.; Nakai, H.; Klene, M.; Li, X.; Knox, J. E.; Hratchian, H. P.; Cross, J. B.; Bakken, V.; Adamo, C.; Jaramillo, J.; Gomperts, R.; Stratmann, R. E.; Yazyev, O.; Austin, A. J.; Cammi, R.; Pomelli, C.; Ochterski, J. W.; Ayala, P. Y.; Morokuma, K.; Voth, G. A.; Salvador, P.; Dannenberg, J. J.; Zakrzewski, V. G.; Dapprich, S.; Daniels, A. D.; Strain, M. C.; Farkas, O.; Malick, D. K.; Rabuck, A. D.; Raghavachari, K.; Foresman, J. B.; Ortiz, J. V.; Cui, Q.; Baboul, A. G.; Clifford, S.; Cioslowski, J.; Stefanov, B. B.; Liu, G.; Liashenko, A.; Piskorz, P.; Komaromi, I.; Martin, R. L.; Fox, D. J.; Keith, T.; Al-Laham, M. A.; Peng, C. Y.; Nanayakkara, A.; Challacombe, M.; Gill, P. M. W.; Johnson, B.; Chen, W.; Wong, M. W.; Gonzalez, C.; Pople, J. A. *Gaussian 03*, revision B.03; Gaussian, Inc.: Wallingford, CT, 2004.
(42) Ahlrichs, R.; Bär, M.; Häser, M.; Horn, H.; Kölmel, C *Chem. Phys. Lett.* **1989**, *162*, 165; current version: http://www.turbomole.de.
(43) Werner, H.-J. A package of ab initio programs. *MOLPRO*, ver. 5;20061; 2006; http://www.molpro.net.
(44) Matsuda, Y.; Ebata, T.; Mikami, N. *J. Chem. Phys.* **1999**, *110*, 8397.
(45) Pliva, J.; Pine, A. S. *J. Mol. Spectrosc.* **1987**, *126*, 82.
(46) Page, R. H.; Shen, Y. R.; Lee, Y. T. *J. Chem. Phys.* **1988**, *88*, 4621.
(47) Henson, B. F.; Hartland, G. V.; Venturo, V. A.; Felker, P. M. *J. Chem. Phys.* **1992**, *97*, 2189.
(48) Erlekam, U.; Frankowski, M.; Meijer, G.; von Helden, G. *J. Chem. Phys.* **2006**, *124*, 171101.
(49) Vargas, R.; Garza, J.; Friesner, R. A.; Stern, H.; Hay, B. P.; Dixon, D. A. *J. Phys. Chem. A* **2001**, *105*, 4963.
(50) Frey, J. A.; Leutwyler, S. *Chimia* **2005**, *59*, 511.
(51) Frey, J. A.; Leutwyler, S. *J. Phys. Chem. A* **2005**, *109*, 6990.
(52) Frey, J. A.; Leutwyler, S. *J. Phys. Chem. A* **2006**, *110*, 12512.
(53) Hatfield, M. P. D.; Palermo, N. Y.; Csontos, J.; Murphy, F.; Lovas, S. *J. Phys. Chem. B* **2008**, *112*, 3503.

JP8110474